HHS Public Access

Author manuscript

J Orthop Res. Author manuscript; available in PMC 2023 October 01.

Osteochondroma formation is independent of heparanase expression as revealed in a mouse model of Hereditary Multiple Exostoses

Christina Mundy[1], **Juliet Chung**[1], **Eiki Koyama**[1], **Stuart Bunting**[2], **Rajeev Mahimkar**[2], **Maurizio Pacifici**[1]

[1]Translational Research Program in Pediatric Orthopaedics, Division of Orthopaedic Surgery, The Children's Hospital of Philadelphia, Philadelphia, Pennsylvania

[2]BioMarin Pharmaceutical, Inc., Novato, California

Abstract

Hereditary Multiple Exostoses (HME) is a rare, pediatric disorder characterized by osteochondromas that form along growth plates and provoke significant musculoskeletal problems. HME is caused by mutations in heparan sulfate (HS)-synthesizing enzymes EXT1 or EXT2. Seemingly paradoxically, osteochondromas were found to contain excessive extracellular heparanase (Hpse) that could further reduce HS levels and exacerbate pathogenesis. To test *Hpse* roles, we asked whether its ablation would protect against osteochondroma formation in a conditional HME model consisting of mice bearing floxed *Ext1* alleles in *Agr-CreER* background (*Ext1*$^{f/f}$*;Agr-CreER* mice). Mice were crossed with a new global *Hpse*-null (*Hpse*$^{-/-}$) mice to produce compound *Hpse*$^{-/-}$*;Ext1*$^{f/f}$*;Agr-CreER* mice. Tamoxifen injection of standard juvenile *Ext1*$^{f/f}$*;Agr-CreER* mice elicited stochastic *Ext1* ablation in growth plate and perichondrium followed by osteochondroma formation, as revealed by micro-computed tomography and histochemistry. When we examined companion conditional *Ext1*-deficient mice lacking *Hpse* also, we detected no major decreases in osteochondroma number, skeletal distribution and overall structure by the analytical criteria above. The *Ext1* mutants used here closely mimic human HME pathogenesis but have not been previously tested for responsiveness to treatments. To exclude some innate therapeutic resistance in this stochastic model, tamoxifen-injected *Ext1*$^{f/f}$*;Agr-CreER* mice were administered daily doses of the retinoid Palovarotene, previously shown to prevent ectopic cartilage and bone formation in other mouse disease models. This treatment did inhibit osteochondroma formation compared to vehicle-treated mice. Our data indicate that heparanase is not a major factor in osteochondroma initiation and accumulation in mice. Possible roles of heparanase upregulation in disease severity in patients are discussed.

Correspondence to: Christina Mundy (matticolac@chop.edu), Rajeev Mahimkar (RMahimkar@bmrn.com) or Maurizio Pacifici (pacificim@chop.edu).

AUTHOR CONTRIBUTIONS

All authors actively participated in the research. CM, JC and EK carried out most of the animal studies. SB created the heparanase-null mice. RM supervised the creation of heparanase-null mice. All authors participated in data analysis and interpretation. RM and MP monitored the project. MP was in charge of writing of the manuscript with active participation by the authors who approved the final manuscript for submission.

Keywords

Heparanase; heparan sulfate; Hereditary Multiple Exostoses; osteochondroma; Palovarotene

1. INTRODUCTION

Hereditary Multiple Exostoses (HME) is a rare, autosomal dominant, musculoskeletal pediatric disorder with an estimated incidence of 1:50,000 individuals worldwide.[1] Known also as Multiple Osteochondroma (MO), HME is characterized by benign tumors (referred to as exostoses or osteochondromas) that develop within perichondrium flanking the growth plate in long bones, ribs and other skeletal elements in children and adolescents. [2–4] The osteochondromas initiate with formation of ectopic cartilage, acquire a growth plate-like structure themselves and elongate outwardly, and undergo endochondral ossification in their proximal region, thus remaining connected to the neighboring osseous elements from which they originate. Because of their large number, size and multiple locations, the osteochondromas can cause a variety of health problems that include skeletal deformities, growth retardation, chronic pain, and impingement of nerves, muscles and vessels.[5; 6] Surgery is used to resect the most symptomatic osteochondromas, but because of their number and challenging anatomical locations, many osteochondromas are left in place, causing life-long problems and increasing the frequency of malignant transformation into osteosarcomas.[7] At present, there is no approved drug treatments to prevent, reduce or reverse the development of osteochondromas.[3; 8]

The majority of HME cases are linked to a loss-of-function heterozygous mutation in the tumor suppressor genes *EXT1* or *EXT2.* [9–12] These genes encode Golgi glycosyltransferases responsible for heparan sulfate (HS) synthesis and assembly onto the core proteins of cell surface and matrix proteoglycans such as syndecans and glypicans.[13–16] Because both EXT1 and EXT2 proteins are needed for efficient HS polymerization, the heterozygous *EXT* mutation carried by HME patients causes a systemic decrease of HS levels of about 50%.[17] Such partial decrease is found to elicit appreciable changes in certain HS-dependent processes such as lipid metabolism in liver,[18] but is thought to be insufficient to cause osteochondroma development on its own.[3] In accordance with general traits and rules of tumorigenesis,[19; 20] osteochondroma development requires a stochastic somatic second hit that would directly or indirectly lead to a further drop in HS levels, rendering local cells virtually devoid of HS.[2; 3] In line with these theses, patient genetic studies did detect loss-of-heterozygosity (LOH), aneuploidy or other chromosomal changes in human osteochondroma surgical retrieval specimens, rendering some local cells *EXT1*- or *EXT2*-null.[21–24] Other studies detected additional genetic changes, including compound heterozygous *EXT1* plus *EXT2* mutations in osteochondromas in the same patient that would be expected to reduce HS levels by about 75%.[25–29] Findings in *Ext* mouse mutants are in agreement with human studies. Whereas global heterozygous loss of *Ext1* or *Ext2* causes minimal phenotypic changes in young mice,[30; 31] conditional homozygous loss of both *Ext1* or *Ext2* alleles as well as compound heterozygous loss of *Ext1* plus *Ext2* causes widespread osteochondroma development, mimicking human HME.[31–33] The overall notion

emerging from human and mouse studies is that osteochondroma formation requires a steep loss of HS in affected local cells, switching their phenotype to tumorigenic.

Intriguingly, previous studies in other cancer types showed that decreases or loss of *EXT* expression and HS production are accompanied by an increase in gene expression of *heparanase (Hpse),* the only vertebrate secreted enzyme that acts on and metabolizes extracellular HS.[34–38] These seemingly paradoxical observations indicate that when HS synthesis is reduced, cancer cells actually up-regulate production of extracellular heparanase to further lower their HS levels and do so in proportion to the degree of their malignancy.[38] The higher heparanase activity is widely thought to facilitate cancer cell proliferation and survival by liberating extracellular HS-bound growth factors[39] and making them bio-available to the cells.[35; 40–42] Interestingly, excessive *Hpse* expression has also been found to occur in osteochondromas from HME patients.[43] We confirmed these trends by immunohistological analysis of human osteochondromas compared to normal surgical discard growth plates, and we found also that experimental reduction of HS levels in cultured cells boosted *Hpse* expression.[44] Together, these previous studies raised the possibility that heparanase could be a culprit in HME pathogenesis. In the present study we tested this important thesis by delineating and comparing osteochondroma formation in conditional stochastic *Ext1*-deficient HME mice[32] bearing or not global *Hpse* ablation.

2. METHODS

2.1 Ethics statement regarding mouse studies

All experiments involving wild type and transgenic mice were reviewed by the IACUC at The Children's Hospital of Philadelphia (protocol no. IAC 14–000952, principal investigator MP). Animals were handled, treated and cared for according to the approved protocols and all procedures fully complied with the ARRIVE guidelines.

2.2 Generation and verification of *Hpse*-null mice

Mice harboring a 905 bp genomic deletion spanning the proximal promoter and exon 1 of the heparanase (*Hpse*) gene were obtained by co-injection of Cas9 mRNA and single guide (sg) RNAs (Table 1) into C57BL/6J fertilized embryos via non-homologous end joining (NHEJ) – mediated repair, using core services provided by Jackson's Laboratories. *Hpse* gene deletions were screened by PCR using primers spanning the target sites (Table 2). Sanger sequencing analysis identified and confirmed mosaic founder mice. These founders were bred to wildtype (WT) C57BL/6J mice (Jackson Labs #664, Bar Harbor, ME) to generate F1 heterozygous progeny for subsequent intercrossing. To confirm the generation of $Hpse^{+/-}$ and $Hpse^{-/-}$ mice, DNA was extracted from tail biopsies, amplified with primers targeting the deleted region and ran under standard PCR electrophoretic conditions. To confirm the absence of *Hpse* gene expression, total RNA was isolated from the liver of WT, $Hpse^{+/-}$ and $Hpse^{-/-}$ mice using TRIzol reagent (Life Technologies, Carlsbad, CA) according to the manufacturer's protocol. Whole RNA was quantified by Nanodrop., and 1 μg aliquots were reversed transcribed using the Verso cDNA synthesis kit (Thermo Fisher Scientific, Waltham, MA). cDNA was amplified using primers and PCR conditions as

described.[45] The amplified products were separated by electrophoresis on a 1% agarose gel and visualized by SYBR Safe DNA gel stain (Invitrogen, Carlsbad, CA).

2.3 Transgenic mouse lines, husbandry and drug treatment

Mice bearing an inducible loss-of-function allele of *Ext1* in which exon 2 is flanked by head-to-head *loxP* sites (heretofore referred to as $Ext1^{f/f}$ mice) were created and described previously[32]. All mice were housed in conventional housing (5 mice per cage) and given unlimited access to food and water. Shepard shacks were added to the cages for environmental enrichment. The mice were mated with $Agr\text{-}CreER^{T2}$ transgenic mice expressing *CreER* recombinase under the control of *aggrecan* enhancer sequences[46] to eventually generate compound $Ext1^{f/f}; Agr\text{-}CreER^{T2}$ mice. $Hpse^{-/-}$ mice were bred to $Ext1^{f/f}; Agr\text{-}CreER^{T2}$ to generate $Ext^{+/f}; Agr\text{-}CreER^{T2};Hpse^{+/-}$ mice. $Hpse^{-/-}$ mice were also bred to $Ext1^{f/f}$ mice to generate $Ext^{+/f};Hpse^{+/-}$ mice that were mated with $Ext^{+/f};Agr\text{-}CreER^{T2};Hpse^{+/-}$ mice to generate experimental $Ext^{f/f};Agr\text{-}CreER^{T2};Hpse^{-/-}$ mice as well as control littermates. At 5 weeks of age, experimental and control mice were given a single intraperitoneal injection of tamoxifen (1 mg/13.3grs per body weight); stock solution was 20 mg/ml in ethanol: corn oil mixture at 1:4 ratio. Mice were euthanized at 6 weeks post tamoxifen injection to assess osteochondroma development. A total number of 3–5 mice were used per group to evaluate phenotype. [47]

For Palovarotene (Atomax Chemicals, ShenZhen, China) treatments, the drug was dissolved in DMSO at 10 mg/ml stock solution. Aliquots were prepared and stored at −20°C. Fresh aliquots were used every two weeks. On the day of treatment, an aliquot was thawed and mixed with the appropriate amounts of DMSO and corn oil to generate a working solution; this was used for two weeks and then replaced with a new one. Sufficient numbers of mice per experiment were placed in separate cages and randomized into control and experimental groups to minimize bias. $Ext1^{f/f};Agr\text{-}CreER^{T2}$ mice were given Palovarotene at 3 mg/kg by oral gavage 5 days per week for 6 weeks. Companion controls were given the vehicle mixture of DMSO and corn oil. Each subgroup contained a minimum of 5 mice per experiment. Treatment started one day after tamoxifen injection. Before gavage, mice were anesthetized by inhalation of 1.5% isoflurane in 98.5% oxygen to minimize discomfort as prescribed by IACUC. Oral gavage probes were 22 gauge and 25 mm long (Instech Laboratories, Plymouth Meeting, PA). After drug administration, animals were regularly monitored for signs of overt toxicity, including lethargy and dystonia, and Institutional LAS personnel provided additional daily animal monitoring and care.

2.4 Micro computed tomography (μCT) and histochemical analyses

Ribs and long bones were fixed for 72 hours in 4% paraformaldehyde, washed with 1X PBS and stored in ethanol for scanning. Ribs and long bones were scanned using a μCT45 scanner (Scanco Medical AG, Switzerland) and analyzed using manufacturer's issued software. Serial 21 μm 2D and 3D images were acquired at 55 kVp energy, 145 μA intensity and integration time of 200 msec. Raw μCT data were compiled into 2D gray scale images. Ribs and long bones were contoured, and binary images were generated using thresholds of 200 and 260, respectively. After imaging procedures, samples were decalcified

and embedded in paraffin. Serial 5 μm sections were stained with safranin-O and fast green and processed for histochemical osteochondroma analyses as described.[47]

2.5 Osteochondroma quantification

Histological images of ribs were loaded into ImageJ software and pixel dimensions were converted to millimeters (mm). Regions of interest were drawn around the bony and cartilaginous areas of the osteochondromas from multiple ribs per animal to measure the areas. Surface areas were analyzed using Prism 9 (GraphPad Software Inc.). Student's t-test and one-way analysis of variance (ANOVA) were used to establish statistical significance. Threshold for significance for all tests was set as $p \leq 0.05$.

3. RESULTS

3.1 Creation and verification of *Hpse*-null mice

As indicated above, heparanase is the only vertebrate secreted enzyme that is responsible for metabolism and cleavage of HS chains present in extracellular and cell surface proteoglycans such as syndecans and perlecan.[35] Because HS cleavage has major functional consequences including liberation of HS-bound growth factors and cytokines and strong cellular responses, *Hpse* is normally expressed by relatively few tissues and is under strict transcriptional regulation.[35; 40–42] To directly test its possible roles in osteochondroma formation during HME, we first set out to create a line of *Hpse*-null mice, expecting it to be viable based on previous studies[45] and thus amenable to be genetically introduced into conditional stochastic HME model mice. The mouse *Hpse* gene comprises 12 exons with the translation start site within exon 1 (MGI: 1343124). Thus, we used a CRISPR/Cas9 approach to specifically target and ablate a 905 base pair segment that comprises the proximal promoter and exon 1 (Figure S1A,B). We obtained mosaic founders that were intercrossed to propagate the mutation. Using PCR primer pairs spanning the entire targeted region (Table 2), we monitored progenies and found that they displayed Mendelian inheritance. Thus, the expected WT DNA amplification product of 1257 bp was appreciable in homozygous WT and heterozygous mutants but not in homozygous mutants (Figure S1C, left panel lanes), while the expected knock-out amplification band of 352 bp was observed in heterozygous and homozygous mutants only (Figure S1C, left panel lanes). To double-check the results, we used a primer pair from within the deleted region itself. The expected amplification product of 485 bp was seen in WT and heterozygous mice only, but not homozygous mutants (Figure S1C, right panel lanes).

Ablation of the 905 bp region spanning the upstream promoter and exon 1 should result not only in lack of gene expression but also absence of alternative transcripts. To make sure this was the case, we isolated total RNA from the liver of WT and homozygous *Hpse* mutant mice above and processed them for cDNA synthesis and RT-PCR, using primer pairs specific for the 5', middle and 3' portions of *Hpse* transcript. Amplification products of expected sizes (332, 330 and 331 bp, respectively) were detected in WT sample but not samples from two knock-out mutants (Figure S1D, WT vs KO 1 and KO 2, left and central panels). As internal control for RNA quality, we used primers for housekeeping ribosomal

protein L19, and an RT-PCR amplification product of 419 bp was elicited by all samples (Figure S1D, far right panel).

3.2 Osteochondromas form in ribs and long bones in both *Ext1*- and *Ext1;Hpse*-null mice

Having obtained an effective *Hpse*-null mouse line, we moved on to test whether this gene has roles in the development and accumulation of osteochondromas in mice. To this end, we relied on an effective transgenic HME mouse model previously created by Jones et al.[32] in which head-to-head *LoxP* sites introduced into the *Ext1* gene lead to conditional *Cre*-induced stochastic loss of normal alleles, thus mimicking stochastic events such as loss-of-heterozygosity (LOH) seen during pathogenesis of osteochondromas in HME patients.[22; 23] Floxed *Ext1* mice were mated with *aggrecan-CreER*^{T2} (*Agr-CreER*^{T2}) mice that elicit tamoxifen-dependent expression of *CreER*^{T2} in growth plate chondrocytes and perichondrial cells normally involved in osteochondroma development.[2] These mice were then mated to *Ext1*$^{+/f}$*;Hpse*$^{-/-}$ mice to ultimately generate compound homozygous *Ext1*$^{f/f}$*;Agr-CreER;Hpse*$^{-/-}$ mice as well as control littermates including *Ext1*$^{+/f}$*;Agr-CreER*, *Ext1*$^{f/f}$*;Agr-CreER*, and *Ext1*$^{f/f}$*;Agr-CreER;Hpse*$^{+/-}$ mice. All mice received a single tamoxifen injection (1 mg/13.3 gr/bw) at 5 weeks and were then monitored over time. Mice were sacrificed after 6 weeks post tamoxifen injection to assess osteochondroma development and growth and to establish similarities and differences amongst the various genetic backgrounds. Given that osteochondromas are most prominent and identifiable in ribs and long bones in mouse models based on previous studies, we focused on these skeletal elements to analyze the phenotypes using μCT. As to be expected, no osteochondromas had developed in conditional heterozygous *Ext1*-deficient mice in ribs (Figure 1A) or long bones (Figure 2A), with their skeletal elements being essentially identical to those in wild type mice (not shown).[47] Prominent osteochondromas had instead formed and accumulated in conditional homozygous *Ext1*-deficient littermates in which the tumors were appreciable at the costochondral junction in ribs (Figure 1B) and along the epiphyseal portions of femur and tibia (Figure 2B, arrowheads), confirming the disease severity in this model. The corresponding portions in control unaffected heterozygous *Ext1*-deficient mice were smooth and even (Figure 2A, arrowheads). When we examined homozygous *Ext1*-deficient mice bearing also a monoallelic and biallelic deletion of *Hpse,* we did not observe any major effect on osteochondroma formation as revealed by μCT (Figure 1C,D; Figure 2C,D), with the osteochondromas appearing to be similar in overall appearance and frequency to those seen in ribs and long bones in companion *Ext1*-deficient mice (Figure 1B and Figure 2B). Because the ablation of *Hpse* had no obvious effects, it was difficult to compare μCT data. Thus, we quantified tumor surface area in *Ext1*-deficient versus double *Ext1*;*Hpse*-deficient mice by histomorphometry (see below).

3.3 Osteochondromas display prominent cartilaginous outgrowth in single and double mutant mice

As indicated above, osteochondroma development starts with formation of ectopic cartilage flanking the growth plate, followed by endochondral ossification. To complement the above μCT analysis of mineralized tissues in mutant mice, ribs and long bones harvested from mouse groups at the 6-week time points as above were decalcified and processed for histochemical staining with Safranin O to delineate presence, structure and organization

of cartilaginous tissues in relation to conditional *Ext1* ablation and *Hpse* co-ablation. As shown in Figure 3, ribs and long bones collected from unaffected conditional heterozygous *Ext1*-deficient mice showed a clear, normal and well defined border between growth plate and adjacent perichondrial and periosteal tissues, with the latter containing typical flat-shaped fibroblastic cells best appreciable at higher magnification (Figure 3E,M). In comparison, the rib border in companion homozygous *Ext1*-deficient mice was occupied by numerous ectopic cartilage cells that were arranged in growth plate-like structures and protruded away into surrounding tissues (Figure 3B,F). The femurs of these mutant mice displayed similar large osteochondromas some of which occupying, and infringing into, the joint space (Figure 3J,N). When we analyzed homozygous *Ext1*-deficient mice with monoallelic and biallelic deletion of *Hpse*, we found that ectopic cartilage formation was as advanced and severe as in companion *Ext1*-deficient mice and was so in both ribs and femurs (Figure 3C,G,K,O and Figure 3D,H,L,P). The data also indicated that there were no obvious differences in chondrocyte organization into growth plate-like structures amongst the different mutants. The surface area of the rib osteochondromas from homozygous *Ext1*-deficient mice and homozygous *Ext1*-deficient mice with monoallelic and biallelic deletion of *Hpse* were quantified by ImageJ (Figure S2).

3.4 Stochastic model HME mice are responsive to drug treatment

The lack of major effects by *Hpse* ablation on osteochondroma development was quite unexpected based on heparanase's reported roles in mechanisms of tumor formation in several other systems.[35] It should be noted that previous studies on potential therapeutic strategies in HME utilized traditional floxed *Ext1* HME mice bearing standard head-to-tail *loxP* sites, eliciting effective *Ext1* ablation in all cells targeted by Cre action.[47; 48] However, the HME model mice used here are stochastic, resemble human HME pathogenesis more closely, but have not been used for testing possible therapeutic strategies. Thus, it became important to clarify whether these mice are actually amenable and responsive to treatment and do not have some intrinsic resistance to it because of their lower degree of *Ext1* ablation after Cre action. Accordingly, we tested whether osteochondroma formation in these stochastic model HME mice could be inhibited by systemic administration of Palovarotene, a drug we previously identified for prevention of heterotopic ossification (HO) in mouse models of the severe pediatric disorder Fibrodysplasia Ossificans Progressiva.[49] HO and osteochondromas share the basic fact that both pathologies start with ectopic cartilage formation followed by endochondral ossification.[50] Stochastic $Ext1^{f/f}$;*Agr-CreER* mice at 5 weeks of age were given a single tamoxifen injection as above and were then treated with Palovarotene (3 mg/kg)[49; 51] or vehicle by oral gavage (5 days/week) for a total of 6 weeks. To assess effects on osteochondroma formation, we collected ribs and long bones from drug- and vehicle-treated mutant mice and subjected them to μCT. Both ribs and long bones in vehicle-treated *Ext1*-deficient mutant mice displayed the expected significant number of osteochondromas (Figure 4A,E; red arrowheads). Instead, there was a clear decrease in osteochondroma formation in Palovarotene-treated mutant mice in both ribs (Figure 4B–D, red arrowheads, triplicate samples) and long bones (Figure 5F–H, red arrowheads, triplicate samples). Following μCT analysis, the samples were decalcified and processed for sectioning and staining with Safranin O. Palovarotene treatment had reduced to the development of the cartilaginous portion of osteochondromas in ribs, tibia and femur

(Figure 5B,C; 5E,F; and 5H,I, respectively) compared to vehicle-treated mutant mice (Figure 5A,D,G) albeit to varying degrees from mouse to mouse but without causing apparent changes or closure of adjacent endogenous growth plates (Figure 5). Measurements of surface area by imaging in specimens from companion untreated and treated mice indicated that the decrease was over 50% and statistically significant (Figure S3).

4. DISCUSSION

Given the essential roles HS and HS-rich proteoglycans play in physiology and pathology, the synthesis, structure, distribution and roles of these macromolecules remain at the center of much research activity.[13; 15] This is reflected also by the number of basic and translational studies on enzymes that metabolize and functionally modify extracellular HS including heparanase and SULF1 and SULF2 and on means by which these activities could be targeted therapeutically.[13; 35; 42] In this vein, the original report of excessive heparanase in human osteochondromas from HME patients at both protein and RNA levels was thus similarly indicative of potential pathogenic role by this enzyme.[43] We confirmed the data subsequently and found also that heparanase was particularly abundant along growth plate perichondrium where the osteochondromas form and grow.[44; 52] In addition, we showed that exogenous recombinant heparanase greatly stimulated pathways such as the bone morphogenetic protein (BMP) signaling likely by releasing HS-bound BMPs. This in turn led to a marked stimulation of chondrogenesis and cartilage formation that are the first differentiation steps in osteochondroma development.[44; 52] Together, these and other observations did suggest that heparanase could be an important culprit in osteochondroma pathogenesis in HME but the data reported here do not lend support to that thesis, at least in the aggressive mouse model used and under the experimental regimens followed here. Thus, the current data do not explain what the excess heparanase levels observed in patient osteochondromas may signify and imply, but the following possibilities can be considered in relation to aspects of HME pathology and severity.

It has long been appreciated that HME disease severity varies greatly from patient to patient, causing minor if any symptoms in some patients to causing severe, debilitating skeletal malformations, joint ankyloses, chronic pain and additional limitations in other patients.[5; 53–55] Perplexingly, this range of severity can occur even within siblings bearing the same germline heterozygous mutation in *EXT1* or *EXT2*. Indeed, over 700 independent mutations in either *EXT* gene have been identified so far in HME patients worldwide; while they invariably are all loss-of-function missense, nonsense, frame shift or splice-site mutations, they have proven to be not useful in establishing definitive genotype-phenotype correlations and predicting disease course and severity.[12; 29; 56] To this day then, the basis for HME pathological variability remains a mystery, but many hypotheses have been put forward, including patient genetic background, disease modifiers and interactions amongst unrelated genes.[57] While the data here indicate that *Hpse* is not a key player in osteochondroma formation in the aggressive mouse model used and its ablation cannot protect against disease progression, the data do not exclude the possibility that heparanase could still be a contributor to disease variability and severity in patients. Presence of excess heparanase was found in the original study by Trebicz-Geffen et al. and confirmed in ours,[43; 52] and together these studies examined about 11 patients. However, there was no

attempt to relate heparanase levels and/or activity to disease severity given the low number of patients. Hence, a dedicated and much larger study could be carried out to address the possibility of a direct relationship between enzyme levels and disease severity. It should be pointed out that osteochondromas in patients are not composed of tumor cells only that have all undergone an additional somatic mutation such as LOH, but are a mixture of tumor cells and normal cells, the latter bearing only the original germline heterozygous *EXT* mutation and recruited into tumor growth.[11; 22] Thus, enzymes such as heparanase could have roles in facilitating recruitment of these more normal cells into tumor growth by reducing their HS levels, exacerbating the disease phenotype in some patients. This mechanism may be less important in mouse models where the *Cre* drivers simultaneously ablate both floxed *Ext* alleles in most/all cells engaged in osteochondroma formation, offering one explanation for the observed lack of effects of *Hpse* ablation reported here.

The basic pathogenic defect in HME is the deficiency of HS, and the ability of such deficiency to cause so many skeletal health problems in most patients reflects the multifaceted and essential roles this glycosaminoglycan has in cell and tissue physiology.[13] It is widely assumed that the HS deficiency renders HS-binding growth factors and cytokines more broadly distributed and available for biological action, undermining normal cellular and tissue mechanisms and eliciting tumor growth.[2; 3] Factors normally interacting with -and bound to- HS include BMPs, activins, hedgehogs and fibroblast growth factors, thus representing the most fundamental and powerful growth factors in the body. These factors all possess a specific HS-binding domain containing basic amino acid residues arranged in Cardin-Weintraub motifs.[39; 58] In recent studies, we showed that these domains are not only distinct in different proteins, but are located in specific locations, including the N- or C-terminal ends of the mature protein or in different regions within the pro-protein.[59; 60] Impressively, these differences are conserved through evolution and for over 300 million years, based on our analysis of genomic databases.[39] Reciprocally, HS is not a mere simple polysaccharide made of repeating disaccharide units, but undergoes multiple and sophisticated modifications during its assembly in the Golgi brought about by a large number of enzymes and producing distinct patterns of sulfation and sugar epimerization. The result of this elaborate synthetic process are HS chains containing successive 8–12 saccharide-long segments each of which with distinct modification patterns and diverse protein binding abilities.[13; 61] It is not clear the extent to which HS chains produced by *EXT* heterozygous mutant cells within and around osteochondromas are structurally different from those made by wild type cells in terms of average length and sugar modifications, possibly resulting in modified protein binding properties.[17; 31] However, what is well established is that heparanase is unique in its ability to cleave HS chains into sizable fragments which in turn can exert distinct biological activities including: ferrying growth factors within the surrounding environment; maintaining factor-factor dimeric interactions and activity; facilitating factor binding to respective cell surface receptors; and modulating factor turnover.[13; 62] It is such HS fragmentation and ensuing functions that could be facilitated by excessive heparanase levels in osteochondromas, influencing tumor growth and pathogenic severity in certain patients. Future studies could tackle these and related questions that when answered, will have important basic and translational medicine significance and relevance.

Supplementary Material

Refer to Web version on PubMed Central for supplementary material.

ACKNOWLEDGEMENTS

This study was supported by grant RO1AR061758 from the National Institute of Arthritis, Musculoskeletal and Skin Diseases at the NIH. We would like to thank Travis Maures for participation and contribution to the creation of *Hpse* mutant mice while at Biomarin.

References

1. Wicklund CL, Pauli RM, Johnston D, et al. 1995. Natural history of hereditary multiple exostoses. . Am J Med Genet 55:43–46. [PubMed: 7702095]
2. Huegel J, Sgariglia F, Enomoto-Iwamoto M, et al. 2013. Heparan sulfate in skeletal development, growth, and pathology: the case of Hereditary Multiple Exostoses. Dev Dyn 242:1021–1032. [PubMed: 23821404]
3. Jones KB. 2011. Glycobiology and the growth plate: Current concepts in Multiple Hereditary Exostoses. J Pediatr Orthop 31:577–586. [PubMed: 21654469]
4. Porter DE, Simpson AHRW 1999. The neoplastic pathogenesis of solitary and multiple osteochondromas. J Pathol 188:119–125. [PubMed: 10398153]
5. Goud AL, de Lange J, Scholtes VA, et al. 2012. Pain, physical and social functioning, and quality of life in individuals with multiple hereditary exostoses in The Netherlands: a national cohort study. J Bone Joint Surg Am 94:1013–1020. [PubMed: 22637207]
6. Stieber JR, Dormans JP. 2005. Manifestations of Hereditary Multiple Exostoses. J Am Acad Orthop Surg 13:110–120. [PubMed: 15850368]
7. Porter DE, Lonie L, Fraser M, et al. 2004. Severity of disease and risk in malignant change in hereditary multiple exostoses. J Bone Joint Surg Br 86:1041–1046. [PubMed: 15446535]
8. Pacifici M. 2018. Hereditary multiple exostoses: Are there new plausible treatment strategies? Expert Opin Orphan Drugs 6:385–391. [PubMed: 31448184]
9. Ahn J, Ludecke HJ, Lindow S, et al. 1995. Cloning of the putative tumour suppressor gene for hereditary multiple exostoses (EXT1). Nat Genet 11:137–143. [PubMed: 7550340]
10. Cheung PK, McCormick C, Crawford BE, et al. 2001. Etiological point mutations in the hereditary multiple exostoses gene EXT1: a functional analysis of heparan sulfate polymerase activity. Am J Hum Genet 69:55–66. [PubMed: 11391482]
11. Hecht JT, Hogue D, Strong LC, et al. 1995. Hereditary multiple exostosis and chondrosarcoma: linkage to chromosome 11 and loss of heterozygosity for EXT-linked markers on chromosome 11 and 8. Am J Hum Genet 56:1125–1131. [PubMed: 7726168]
12. Wuyts W, Van Hul W. 2000. Molecular basis of multiple exostoses: mutations in the EXT1 and EXT2 genes. Hum Mutat 15:220–227. [PubMed: 10679937]
13. Bishop JR, Schuksz M, Esko JD. 2007. Heparan sulphate proteoglycans fine-tune mammalian physiology. Nature 446:1030–1037. [PubMed: 17460664]
14. Esko JD, Selleck SB. 2002. Order out of chaos: assembly of ligand binding sites in heparan sulfate. Annu Rev Biochem 71:435–471. [PubMed: 12045103]
15. Iozzo RV, Schaefer L. 2015. Proteoglycan form and function: a comprehensive nomenclature for proteoglycans. Matrix Biol 42:11–55. [PubMed: 25701227]
16. McCormick C, Duncan G, Goutsos KT, et al. 2000. The putative tumor suppressors EXT1 and EXT2 form a stable complex that accumulates in the Golgi complex and catalyzes the synthesis of heparan sulfate. Proc Natl Acad Sci USA 97:668–673. [PubMed: 10639137]
17. Anower-E-Khuda MF, Matsumoto K, Habuchi H, et al. 2013. Glycosaminoglycans in the blood of hereditary multiple exostoses patients: half reduction of heparan sulfate to chondroitin sulfate ratio and the possible diagnostic application. Glycobiology 23:865–876. [PubMed: 23514715]

18. Mooij HL, BernelotMoens SJ, Gordts PL, et al. 2015. Ext1 heterozygosity causes a modest effect on postprandial lipid clearance in humans. J Lipid Res 56:665–673. [PubMed: 25568062]
19. Knudson A. 1971. Mutation and cancer: statistical study of retinoblastoma. Proc Natl Acad Sci USA 68:820–823. [PubMed: 5279523]
20. Knudson AG. 1996. Hereditary cancer: two hits revisited. J Cancer Res Clin Oncol 122:135–140. [PubMed: 8601560]
21. Bernard MA, Hall CE, Hogue DA, et al. 2001. Diminshed levels of the putative tumor suppressor proteins EXT1 and EXT2 in exostosis chondrocytes. Cell Motil Cytoskeleton 48:149–162. [PubMed: 11169766]
22. Bovee JV, Cleton-Jansen A-M, Wuyts W, et al. 1999. EXT-mutation analysis and loss of heterozygosity in sporadic and hereditary osteochondromas and secondary chondrosarcoma. Am J Hum Genet 65:689–698. [PubMed: 10441575]
23. Hameetman L, Szuhai K, Yavas A, et al. 2007. The role of EXT1 in nonhereditary osteochondroma: identification of homozygous deletions. J Natl Cancer Inst 99:396–406. [PubMed: 17341731]
24. Reijnders CM, Waaijer CJ, Hamilton A, et al. 2010. No haploinsufficiency but loss of heterozygosity for EXT in multiple osteochondromas. Am J Path 177:1946–1957. [PubMed: 20813973]
25. Hall CR, Cole WG, Haynes R, et al. 2002. Reevaluation of a genetic model for the development of exostoses in hereditary multiple exostosis Am J Med Genet 112:1–5. [PubMed: 12239711]
26. Ishimaru D, Gotch M, Takayama S, et al. 2016. Large-scale mutational analysis in the EXT1 and EXT2 genes for Japanese patients with multiple osteochondromas. BMC Genetics 17:52. [PubMed: 26961984]
27. Jennes I, Pedrini E, Zuntini M, et al. 2009. Multiple osteochondromas: mutation update and description of the multiple osteochondromas mutation database (MOdb). Hum Mutat 30:1620–1627. [PubMed: 19810120]
28. Sarrion P, Sangorrin A, Urreizti R, et al. 2013. Mutations in the EXT1 and EXT2 genes in Spanish patients with multiple osteochondromas. Scientic Reports 3:1346.
29. Zuntini M, Pedrini E, Parra A, et al. 2010. Genetic models of osteochondroma onset and neoplastic progression: evidence for mechanisms alternative to EXT genes inactivation. Oncogene 29:3827–3834. [PubMed: 20418910]
30. Stickens D, Zak BM, Rougier N, et al. 2005. Mice deficient in Ext2 lack heparan sulfate and develop exostoses. Development 132:5055–5068. [PubMed: 16236767]
31. Zak BM, Schuksz M, Koyama E, et al. 2011. Compound heterozygous loss of Ext1 and Ext2 is sufficient for formation of multiple exostoses in mouse ribs and long bones. Bone 48:979–987. [PubMed: 21310272]
32. Jones KB, Piombo V, Searby C, et al. 2010. A mouse model of osteochondromagenesis from clonal inactivation of Ext1 in chondrocytes. Proc Natl Acad Sci USA 107:2054–2059. [PubMed: 20080592]
33. Matsumoto K, Irie F, Mackem S, et al. 2010. A mouse model of chondrocyte-specific somatic mutation reveals a role for Ext1 loss of heterozygosity in multiple hereditary exostoses. Proc Natl Acad Sci USA 107:10932–10937.
34. Hulett MD, Freeman C, Hamdorf BJ, et al. 1999. Cloning of mammalian heparanase: an important enzyme in tumor invasion and metastasis. Nat Med 5:183–187. [PubMed: 9930866]
35. Jayatilleke KM, Hulett MD. 2020. Heparanase and the hallmarks of cancer. J Translat Med 18:453.
36. Quiros RM, Rao G, Plate J, et al. 2006. Elevated serum heparanase-1 levels in patients with pancreatic carcinoma are associated with poor survival. Cancer 106:532–540. [PubMed: 16388520]
37. Sanderson RD, Elkin M, Rapraeger AC, et al. 2017. Heparanase regulation in cancerm autophagy and inflammation: new mechanims and targets of therapy. FEBS J 284:42–55. [PubMed: 27758044]
38. Zetser A, Bashenko Y, Miao HQ, et al. 2003. Heparanase affects adhesive and tumorigenic potential of human glioma cells. Cancer Res 63:7733–7741. [PubMed: 14633698]

39. Billings PC, Pacifici M. 2015. Interactions of signaling proteins, growth factors and other proteins with heparan sulfate: mechanisms and mysteries. Connect Tissue Res 56:272–280. [PubMed: 26076122]
40. Hanahan D, Weinberg RA. 2011. Hallmarks of cancer: the next generation. Cell 144:646–674. [PubMed: 21376230]
41. Sarrazin S, Lamanna WC, Esko JD. 2011. Heparan sulfate proteoglycans. Cold Spring Harb Perspec Biol 3:a004952.
42. Hammond E, Khurana A, Shridhar V, et al. 2014. The role of heparanase and sulfatases in the modification of heparan sulfate proteoglyacns within thetumor microenvironment and opportunities for novel cancer therapies. Fron Oncol 4:195.
43. Trebicz-Geffen M, Robinson D, Evron Z, et al. 2008. The molecular and cellular basis of exostosis formation in hereditary multiple exostoses. Int J Exp Path 89:321–331. [PubMed: 18452536]
44. Huegel J, Enomoto-Iwamoto M, Sgariglia F, et al. 2015. Heparanase stimulates chondrogenesis and is up-regulated in human ectopic cartilage. A mechanism possibly involved in Hereditary Multiple Exostoses. Am J Path 185:1676–1685. [PubMed: 25863260]
45. Zcharia E, Jia J, Zhang X, et al. 2009. Newly generated heparanase knock-out mice unravel co-regulation of heparanase and matrix metalloproteinases. PLoS ONE 4:e5181.
46. Henry SP, Jang CW, Deng JM, et al. 2009. Generation of aggrecan-CreERT2 knockin mice for inducible Cre activity in adult cartilage. Genesis 47:805–814. [PubMed: 19830818]
47. Sinha R, Mundy C, Bechtold T, et al. 2017. Unsuspected osteochondroma-like outgrowths in the cranial base of Hereditary Multiple Exostoses patients and modeling and treatment with a BMP antagonist in mice. PLoS Genetics 13:e1006742.
48. Inubushi T, Lemire I, Irie F, et al. 2018. Palovarotene inhibits osteochondroma formation in a mouse model of multiple hereditary exostoses. J Bone Min Res 33:658–666.
49. Shimono K, Tung W-E, Macolino C, et al. 2011. Potent inhibition of heterotopic ossification by nuclear retinoic acid receptor-γ agonists. Nature Med 17:454–460. [PubMed: 21460849]
50. Pacifici M. 2018. Retinoid roles and action in skeletal development and growth provide the rationale for an ongoing heterotopic ossification prevention trial. Bone 109:267–275. [PubMed: 28826842]
51. Chakkalakal SA, Uchibe K, Convente MR, et al. 2016. Palovarotene inhibits heterotopic ossification and maintains limb mobility and growth in mice with the human ACVR1R206H Fibrodysplasia Ossificans Progressiva (FOP) mutation. J Bone Min Res 31:1–10.
52. Huegel J, Mundy C, Sgariglia F, et al. 2013. Perichondrium phenotype and border function are regulated by Ext1 and heparan sulfate in developing long bones: A mechanism likely deranged in Hereditary Multiple Exostoses. Dev Biol 377:100–112. [PubMed: 23458899]
53. Alvarez C, De Vera MA, Heslip TR, et al. 2007. Evaluation of the anatomical burden of patients with hereditary multiple exostoses. Clin Orth Relat Res 462:73–79.
54. Clement ND, Duckworth AD, Baker AD, et al. 2012. Skeletal growth patterns in hereditary multiple exostoses: a natural history. J Pediatr Orthop B21:150–154.
55. Clement ND, Porter DE. 2014. Hereditary multiple exostoses: anatomical distribution annd burdern of exostoses is dependent upon genotype and gender. Scottish Med J 59:34–44.
56. Pedrini E, Jennes I, Tremosini M, et al. 2011. Genotype-phenotype correlation study in 529 patients with Hereditary Multiple Exostoses: identification of “protective” and “risk” factors. J Bone Joint Surg 93:2294–2302. [PubMed: 22258776]
57. Pacifici M. 2017. Hereditary Mutliple Exostoses: new insights into pathogenesis, clinical complications, and potential treatments. Curr Osteoporos Rep 15:142–152. [PubMed: 28466453]
58. Cardin AD, Weintraub HJ. 1989. Molecular modeling of protein-glycosaminoglycan interactions. Arterioschler Thromb Vasc Biol 9:21–32.
59. Billings PC, Yang E, Mundy C, et al. 2018. Domains with highest heparan sulfate-binding affinity reside at opposite ends in BMP2/4 versus BMP5/6/7: Implications for function. J Biol Chem 293:14371–14383.
60. Yang E, Mundy C, Rappaport EF, et al. 2019. Identification and characterization of a novel heparan sulfate-binding domain in Activin A longest variants and implications for function. PLOS One 14:e0222784.

61. Bulow HE, Hobert O. 2006. The molecular diversity of glycosaminoglycans shapes animal development. Annu Rev Cell Dev Biol 22:375–407. [PubMed: 16805665]

62. O'Callaghan P, Zhang X, Li J-P. 2018. Heparan sulfate proteoglycans as relays of neuroinflammation. J Histochem Cytochem 66:305–319. [PubMed: 29290138]

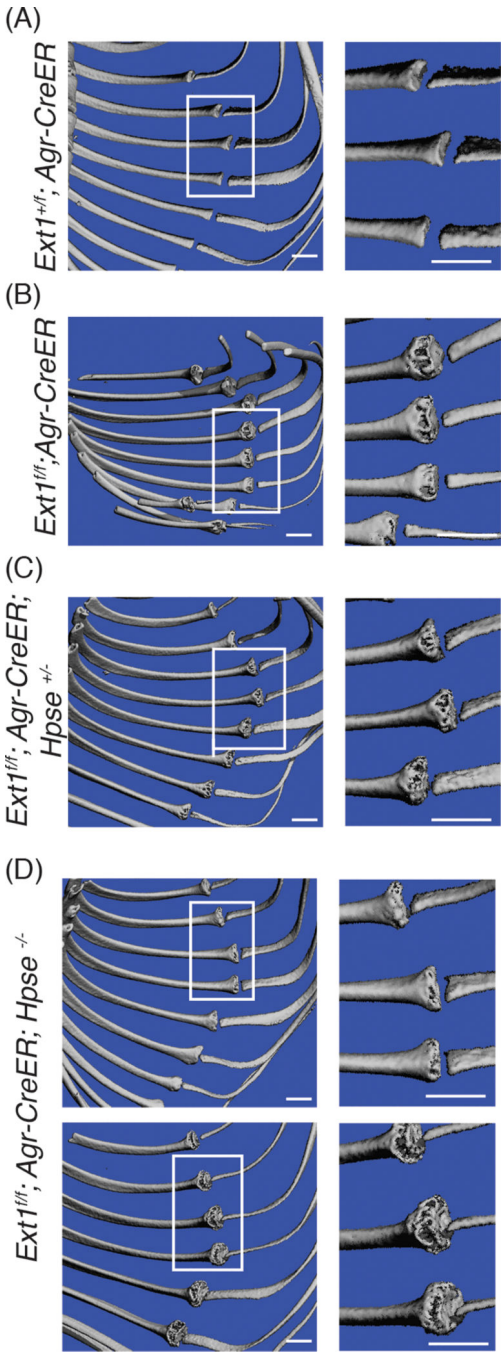

FIGURE 1.

Analysis of osteochondroma formation in ribs of control and mutant mice. (A) Representative μCT image of rib cage from control heterozygous *Ext1*$^{+/f}$*;Agr-CreER* mice that were sacrificed 6 weeks after tamoxifen injection. White box area on left panel identifies the osteochondral junction in neighboring ribs shown at higher magnification on the right panel. Note the characteristic asymmetric bone tissue flanking the growth plate that is translucent by μCT (arrowheads). (B-C) Rib cage images from standard *Ext1*-deficient mice (B, *Ext1*$^{f/f}$*;Agr-CreER*) and *Ext1*-deficient mice in heterozygous *Hpse*-

null background (C, *Ext1*$^{f/f}$*;Agr-CreER;Hpse*$^{+/-}$). Note the conspicuous osteochondromas around the osteochondral junction in all mice, best appreciable in the higher magnification panels on the right (B,C, arrowheads). (D) Ribs from mutant *Ext1*$^{f/f}$*;Agr-CreER;Hpse*$^{-/-}$ mice displaying prominent osteochondromas despite homozygous genetic ablation of *Hpse*. Scale bar: 1 mm. n = 3 *Ext1*$^{+/f}$*;Agr-CreER* , n = 3 *Ext1*$^{f/f}$*;Agr-CreER,* n = 3 *Ext1*$^{f/f}$*;Agr-CreER;Hpse*$^{+/-}$ and n = 5 *Ext1*$^{f/f}$*;Agr-CreER;Hpse*$^{-/-}$.

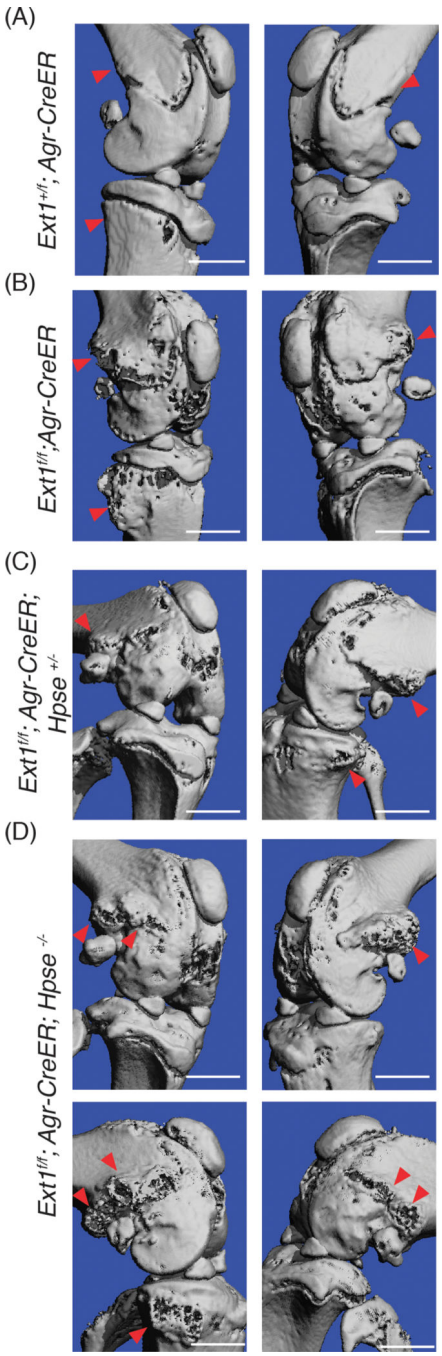

FIGURE 2.

Osteochondroma formation in the knees in control and mutant mice. (A) Representative μCT image of the knee from control heterozygous *Ext1*$^{+/f}$*;Agr-CreER* mice that were sacrificed 6 weeks after tamoxifen injection. Red arrowheads point to normal anatomical characteristics of femur and tibia. (B-C) Representative images of knees from conditional Ext1-deficient mice without and with heterozygous *Hpse* ablation (*Ext1*$^{f/f}$*;Agr-CreER* and *Ext1*$^{f/f}$*;Agr-CreER;Hpse*$^{+/-}$ mice) 6 weeks after tamoxifen injection, respectively. Note prominent osteochondromas protruding from femur and tibia depicted by red arrowheads

in all mice. (D) Representative images of knees from 2 compound *Ext1*-deficient mice with homozygous *Hpse* ablation (*Ext1*$^{f/f}$*;Agr-CreER;Hpse*$^{-/-}$ mice) 6 weeks after tamoxifen injection. Note the large osteochondromas along femur and tibia (red arrowheads) that appear quite similar to those in mutant knees shown in B-C. Scale bar: 1 mm. n = 3 *Ext1*$^{+/f}$*;Agr-CreER*, n = 3 *Ext1*$^{f/f}$*;Agr-CreER,* n = 3 *Ext1*$^{f/f}$*;Agr-CreER;Hpse*$^{+/-}$ and n = 5 *Ext1*$^{f/f}$*;Agr-CreER;Hpse*$^{-/-}$.

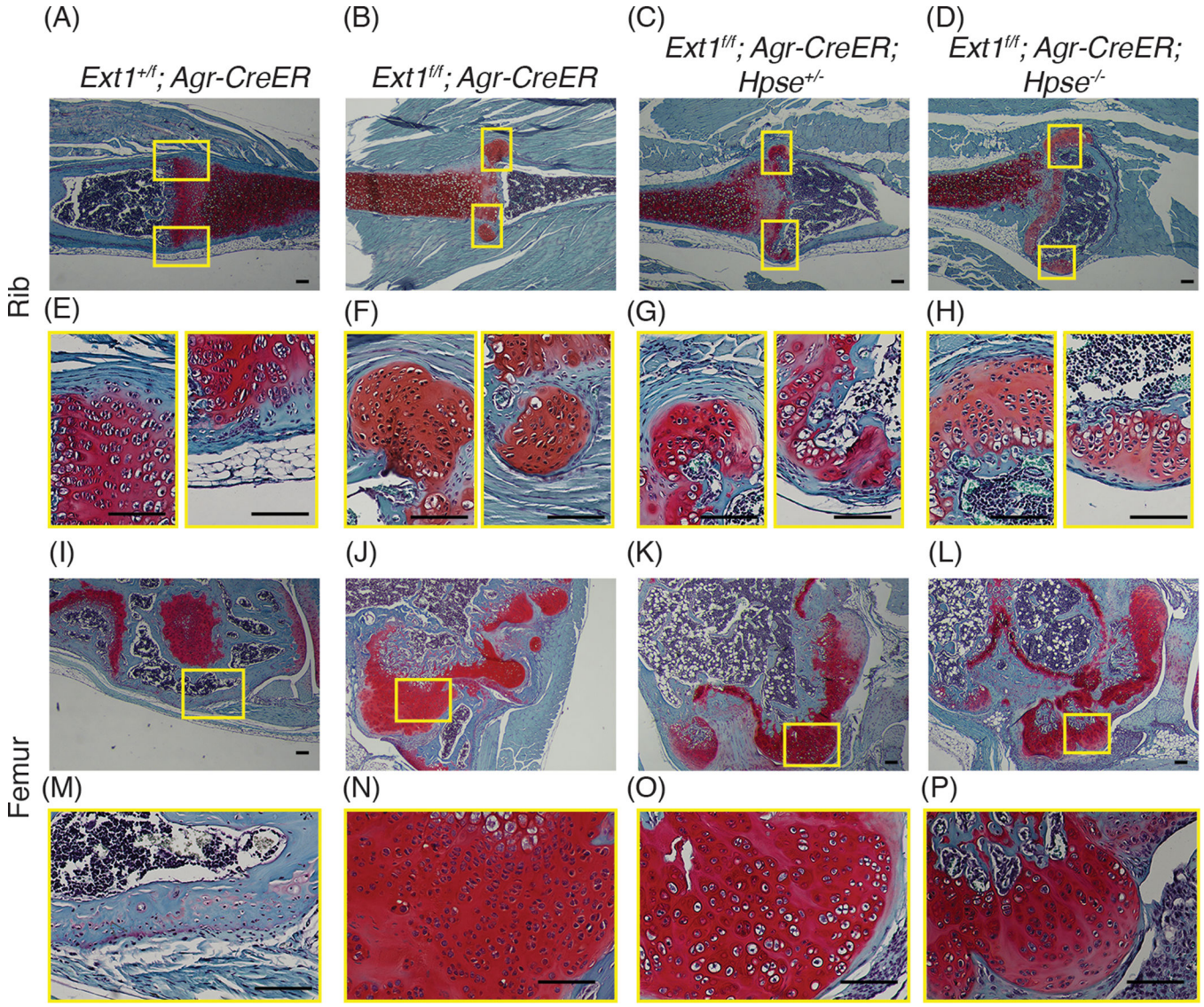

FIGURE 3.

Histochemical examination of osteochondromas in ribs and long bones. (A-D) and (E-H) Longitudinal sections of osteochondral rib junctions in control and mutant mice at 6 weeks post injection stained with safranin O and fast green. Box areas in A-D are shown at higher mag in E-H. In control heterozygous *Ext1*$^{+/f}$*;Agr-CreER* mice, note that the border along growth plate and perichondrium is even and normal (A,E). However, in homozygous *Ext1*-deficient mice bearing heterozygous or homozygous *Hpse* loss (B-D and F-H), the border displays prominent osteochondromas in all genotypes. (I-L) and (M-P) Longitudinal sections of femurs in control and mutant mice at 6 weeks post injection stained with safranin O and fast green. In controls (I,M), the growth plate and perichondrium are typical and smooth. However, in all mutants (J-L and N-P), there are prominent osteochondromas protruding out of growth plate. Boxed areas in I-L are shown at higher mag in M-P. Scale bar: 100 μm. n = 3 *Ext1*$^{+/f}$*;Agr-CreER*, n = 3 *Ext1*$^{f/f}$*;Agr-CreER,* n = 3 *Ext1*$^{f/f}$*;Agr-CreER;Hpse*$^{+/-}$ and n = 3 *Ext1*$^{f/f}$*;Agr-CreER;Hpse*$^{-/-}$.

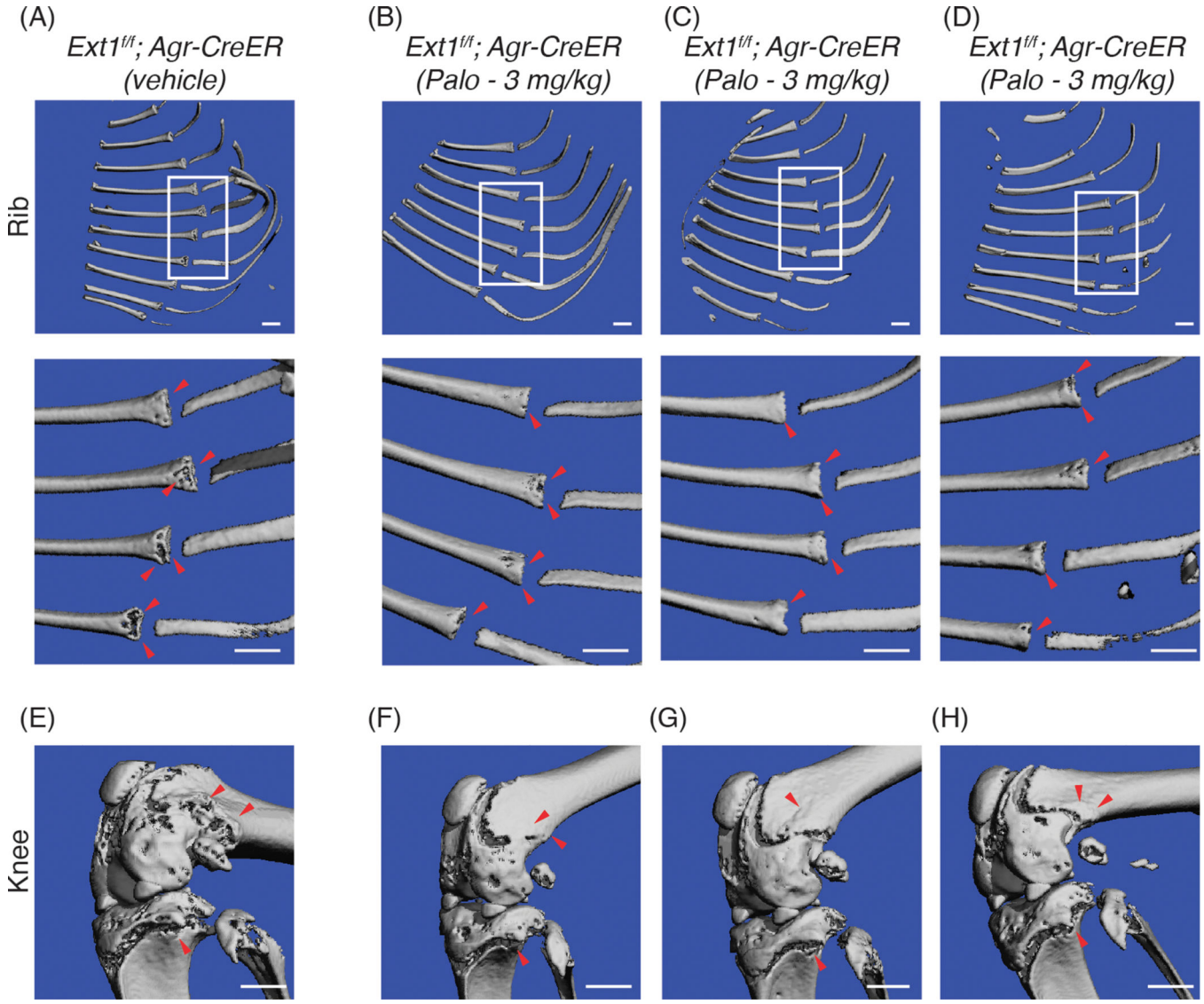

FIGURE 4.

Analysis of osteochondroma formation after Palovarotene administration. (A-D) Representative μCT images of rib cages from vehicle- and Palovarotene-treated *Ext1*-deficient (*Ext1*$^{f/f}$*;Agr-CreER*) mice at 6 weeks after tamoxifen injection. In vehicle-treated mouse (A), large typical osteochodromas are present at the costochondral junction, better visible in white boxed area shown at higher magnification in lower panel (red arrowheads). In companion Palovarotene-treated mice (B-D), there is a clear decrease in osteochondroma formation best appreciable in higher magnification images (lower panels, red arrowheads). Data are from 3 mice to demonstrate consistency of observations. (E-H) Representative μCT images of knees from vehicle- and Palovarotene-treated *Ext1*-deficient (*Ext1*$^{f/f}$*;Agr-CreER*) mice at 6 weeks after tamoxifen injection. Prominent osteochondromas in femur and tibia in vehicle-treated mice (E, red arrowheads) are clearly decreased after Palovarotene treatment (F-H, red arrowheads). Data are from 3 mice to demonstrate consistency of observations. Scale bar: 100 μm. n = 4 vehicle-treated and n = 5 palovarotene-treated mice per group.

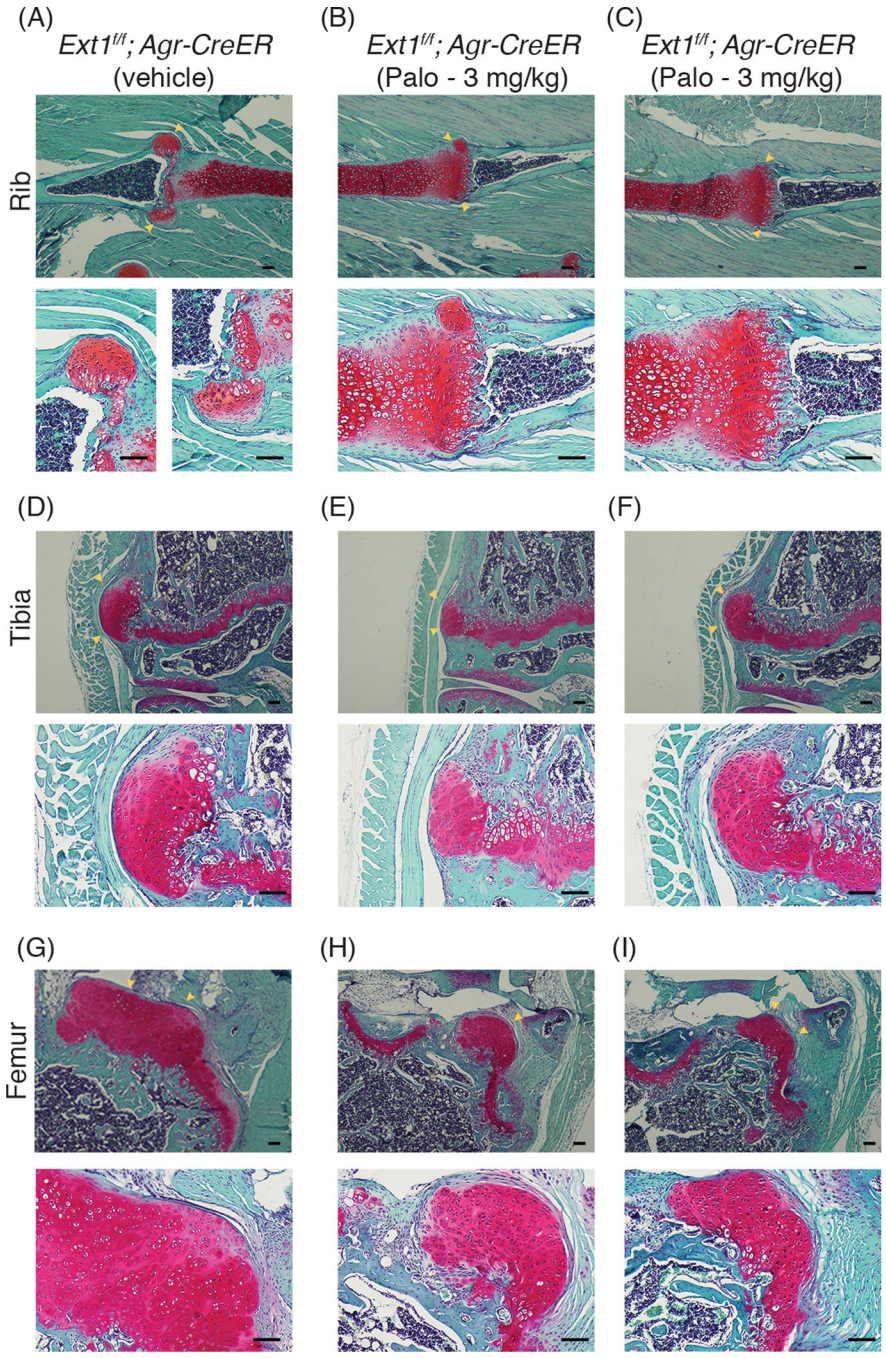

FIGURE 5.

Histochemical analysis of osteochondroma formation after Palovarotene administration. (A,D,G) Sections stained with safranin O and fast green shown at higher mag in lower panels. Note the sizable osteochondromas present at the rib osteochondral junction (A, arrowheads) and along tibia and femur growth plates (D,G, arrowheads) in vehicle treated *Ext1*-deficient mice at 6 weeks after tamoxifen injection. (B-C, E-F and H-I) Sections stained with safranin O and fast green shown at higher mag in lower panels. Note the reduced sizes of cartilaginous osteochondroma areas after Palovarotene treatment in

companion *Ext1*-deficient mice. Data from two mice are shown to demonstrate overall consistency of response, albeit with some variability from mouse to mouse. Scale bar: 100 μm.

n = 4 vehicle-treated and n = 5 Palovarotene-treated mice per group.

TABLE 1

Primers for single guide RNAs used to delete the targeted *Hpse* region

Location	Sequences
Upstream Guides	HpsePro_sgRNA1:AGAAATCGGTCCTTGCACGG HpsePro_sgRNA2:ATCACCACCACCCCCGTGCA HpsePro_sgRNA3:TAGAAATCGGTCCTTGCACCG
Intron 1 Guides	HpseInt1_sgRNA1:CCTGTCCAATCACACACTCGCG HpseInt1_sgRNA2:CTGTCCAATCACACTCGCGA

The indicated single guide (sg) RNAs were co-injected along with Cas9 mRNA into C57BL/6J fertilized embryos to elicit non-homologous end joining-mediated repair and deletion of 905 bp genomic segment spanning *Hpse* proximal promoter and exon 1.

TABLE 2

Primer pairs to genotype *Hpse* mouse mutants

Primer*	**Sense (5'−3')**	**Antisense (5'−3')**	**Length (bp)**
Hpse	GGGTTGCTCAGGATTCCAAG	GGCTCCAGACAAAGTGCTAAG	WT:1257 KO: 352
Deleted region	CCAATGCTCGGATCA	CCAGGACTCAGTACC	485

* Primers in top row flank the targeted deleted *Hpse* region and generate a 1257 bp product in WT and a 352 bp product in knock-out mice by PCR. Primers in lower row are from within the deleted region itself and generate a PCR product of 485 bp in WT and heterozygous mice.